Journal of Materials Chemistry A

Accepted Manuscript

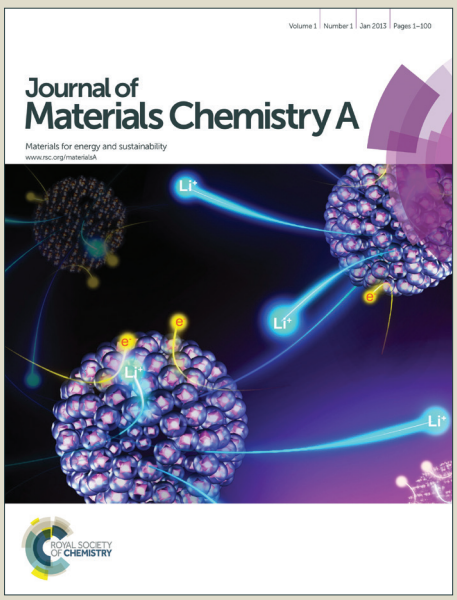

ROYAL SOCIETY OF CHEMISTRY

www.rsc.org/materialsA

Journal Name

RSCPublishing

ARTICLE

Fabrication of core-shell structured mesoporous silica nanospheres with dually oriented-mesochannels through pore engineering

Juan Peng,[ab] Jia Liu,[a] Jian Liu,[c] Yan Yang,[a] Can Li*[a] and Qihua Yang*[a]

Cite this: DOI: 10.1039/xoxxoooooox

Received ooth January 2012,
Accepted ooth January 2012

DOI: 10.1039/xoxxoooooox

www.rsc.org/

This work focuses on engineering the pore orientation and pore size of mesoporous silica nanospheres (MSNs) in one pot. Core-shell structured MSNs possessing dual mesochannel orientation in one particle and tunable larger mesopores (3.0~7.3 nm) have been synthesized by using cetyltrimethyl ammonium bromide (CTAB) as template with the aid of 1,3,5-trimethylbenzene (TMB). The formation of penetrating and radial mesochannels respectively in the core and shell has been characterized by scanning electron microscopy , transmission electron microscopy, N_2 sorption techniques, and further confirmed by the two-step adsorption and desorption curves for lysozyme. Moreover, the pore size, core size and shell thickness of dual oriented MSNs could be easily tunned by varying the TMB content and the synthesis temperature. The mechanism investigations suggest that initially formed silicate species with penetrating channels act as nucleus for the radial arrangement of the cylindrical micelles for the formation of dually oriented-mesostructures, in which TMB could control the pore orientation and pore diameter through affecting the kinetics of silica solid formation and swelling the CTAB micelles.

Introduction

Thanks to the well developed supramolecular assembly and sol-gel chemistry, a big family of the mesoporous silicas with various pore structures and morphologies has been successfully established in the past decade. [1-7] Among them, mesoporous silica nanospheres (MSNs) have attracted substantial attention in the field of catalysis, bioimaging for diagnostics, and nanomedicine, due to their tunable pore sizes, high internal surface area and pore volume, colloidal stability, biocompatibility and short diffusion length. Great efforts have been devoted to tailor the particle morphology,[8] pore size[9] and orientation[10, 11] because these parameters are of particular importance for practical applications of MSNs.

Most MSNs reported so far are with 2-D hexagonal mesostructure and pore diameter less than 3 nm, which were synthesized using cationic surfactant as a soft template in basic medium.[12, 13] For enlarging the pore diameter and tuning the porous structure, dual surfactant system composed of non-ionic triblock copolymer surfactant and cationic fluorocarbon surfactant was developed for the synthesis of MSNs with 3-D cubic or foam-like porous structure and pore diameter in the range of 5 to 30 nm in a weak acidic system.[14, 15] Shi and co-workers[16] reported the synthesis of core-shell structured dual-mesoporous silica spheres with smaller mesopores in the shell and larger mesopores in the core by utilizing an amphiphilic block copolymer (polystyrene-b-poly (acrylic acid), PS-b-PAA) and cetyltrimethyl ammonium bromide (CTAB) as cotemplates. Recently, MSNs containing both cubic and hexagonally structured compartments within one particle were reported by Wiesner and co-workers.[17] In addition to the pore size and porous structure, the pore orientation affects greatly the diffusion of guest molecules through MSNs.[18-20] However, most MSNs reported have penetrating mesochannels throughout the opposite poles of the sphere.[12] Several groups attempted to synthesize MSNs with radial-orientated pore system (so called stellate-like channel) using microemulsion media[21] or employing cationic surfactant as soft template with the aid of small organic amines[22]. For instance,[11] MSNs with controlled mesochannel orientation (i.e., straight, helical, and radial nanopores) were synthesized with the aid of an organosilane, but the pore diameter is only ~2 nm. Combining penetrating and radial pore in one particle would provide more chances for modulating the diffusion kinetics of guest molecules, especially for macromolecules, such as enzyme, which faces higher transfer resistance and calls for larger pore cavity. However, it still remains a challenge to control the pore size, orientation and mesostructures simultaneously. It is desirable to synthesize MSNs containing different pore

orientation, size and structures in one particle for specific chemistries in catalysis or drug delivery.

In this paper, we report the one pot synthesis of core-shell structured MSNs with controlled pore orientation (penetrating and radial pores), pore size (3.0 to 7.3 nm), and mesostructure (2-D hexagonal and 3-D cage-like) in one particle. With the aid of 1,3,5-trimethylbenzene (TMB), MSNs possessing penetrating and radial mesochannels in the core and shell respectively are obtained by controlling the kinetics of hydrolysis and condensation of tetraethyl orthosilicate (TEOS) around cetyltrimethyl ammonium bromide (CTAB) in basic medium. The MSNs with dually oriented-mesochannels exhibit unique two-step adsorption-desorption profiles in lysozyme adsorption, along with the increased adsorption capability and cumulative release quantity due to the large pore size. It could be expected that the dually oriented MSNs would have potential applications in the field of biocatalysis and drug delivery.

Experimental Section

Chemicals and reagents

All of the reagents were of analytical grade and used as received without further purification. Cetyltrimethylammonium bromide (CTAB) were purchased from Sigma-Aldrich Company Ltd (USA). Tetraethoxysilane (TEOS) and ethyl acetate were obtained from Sinopharm Chemical Reagent Co., Ltd. TMB was obtained from Tianjing Guangfu Institute of Fine Chemical Industry. Lysozyme (LYZ) was commercially available from Dalian Chenyu Biochemical Reagents Co. and stored at 4 ^{o}C before being used. Other reagents were purchased from Shanghai Chemical Reagent, Inc. of the Chinese Medicine Group.

Synthesis of core-shell structured MSNs with different pore sizes

The MSNs possessing dually oriented mesochannel and large pore size were synthesized using cationic surfactant, CTAB, as soft template and TEOS as silicate source with the aid of TMB in basic medium. In a typical synthesis, CTAB (0.1g) was added to an aqueous solution (45 ml) of NaOH (0.35 mL, 2 M). After dissolution of CTAB, a proper amount of TMB was added to the system. The mixture was sonicated for one hour for the formation of stable white emulsion. TEOS (0.5 mL) was added followed by the addition of ethyl acetate (0.4 mL). The final chemical composition of the precursor solution was 1 CTAB : 2.6 NaOH : x TMB : 8.2 TEOS : 9110 H_2O (molar ratio). Then the mixture was stirred for two hours at the given temperature. After cooling to room temperature, the powder product was isolated by filtration, washed with distilled water and air-dried for 24 h. The as-synthesized material was then calcined at 550 ^{o}C for six hours in air. The final product was denoted as MSN-x-T, where x was the molar ratio of TMB/CTAB and T is the synthesis temperature.

Lysozyme (LYZ) adsorption

LYZ solution with a concentration of 200 μmol/L were prepared by dissolving 288 mg LYZ in sodium carbonate buffer solution (10 mM, pH = 10.8). In a typical adsorption process, the MSNs material was divided into 10 copies. Each one contains 10 mg of MSNs, suspended in the LYZ solution of 2 mL. The resulting mixtures were continuously shaken with a speed of 160 rpm at 20 °C for 79 h, and was successively taken out at different times. Thereafter, the supernatant and solid material were separated by centrifugation. The concentration of LYZ was measured by UV-vis spectrophotometer at a wavelength of 280 nm, and the amount of LYZ loaded onto the MSN was calculated by subtracting LYZ in the supernatant from the total LYZ amount. As for the experiments dealing with the desorption behavior of LYZ loaded on MSNs, 25 mg of LYZ@MSN was suspended in the buffer solution (35 mL, pH = 10.8). During the desorption process, samples (2 mL) were withdrawn periodically and centrifuged. After the supernatant was collected for UV-vis detection, another equivalent buffer solution (2 mL) was added into the system, together with the withdrawn MSNs materials.

Characterization

N_2 sorption isotherms were carried out on a Micromeritics ASAP2020 volumetric adsorption analyzer. Before the sorption measurements, samples were out-gassed at 393 K for six hours. X-Ray powder diffraction (XRD) patterns were recorded on a Rigaku RINT D/Max-2500 powder diffraction system using Cu Kα radiation (λ=0.1541 nm). Transmission electron microscopy (TEM) was performed using HITACHI HT7700 at an acceleration voltage of 100 kV. Scanning electron microscopy (SEM) was performed on HITACHI S5500. Dynamic light scattering (DLS) was carried out on Malvern zetasizer nano ZS90 manufactured by Malvern instruments corporate with the test temperature of 20 ^{o}C. UV-vis spectra were collected with a Shimadazu UV-2550 spectrometer. C, H, and N elemental analysis was performed on a varioEL III apparatus. X-ray photoelectron spectroscopy (XPS) was recorded on VG ESCALAB MK2 apparatus using Al Kα (hλ=1486.6 eV) as the excitation light source.

Results and discussion

Characterization of MSNs

The mesoporous silica nanospheres were denoted as MSN-x-T, where x was the molar ratio of TMB/CTAB and T is the synthesis temperature. The transmission electron microscopy (TEM) image and scanning electron microscopy (SEM) image show that MSN-7.5-40 mainly consisted of mono-dispersed spheres with relatively broad particle size distribution (Figure 1). Si element EDX further confirms that the sample is the solid particle (Figure S1). The nanosphere has core-shell structure with penetrating mesochannels in the "core" region and radial mesochannels in the "shell" region. Estimated from the TEM image, MSN-7.5-40 has the same pore diameter in the shell and in the core of ~7 nm, and the average particle size of 250 nm

with the core diameter to shell diameter ratio of about 1. Particle size distribution determined by dynamic light scattering (DLS) technique is centered at 256 nm (Figure S2). The larger particle size obtained by DLS than that by TEM characterization is due to the solvation effect for MSNs in solution. The nitrogen sorption isotherm of MSN-7.5-40 exhibits type IV isotherm pattern with H2 hysteresis loop characteristic of cage-like mesopores (Figure 1C). The pore size distribution centered at 7.3 nm, showing that the sample has only one set of mesopore, which is consistent with the TEM results. The BET surface area and pore volume are 765 m^2/g and 1.34 cm^3/g, respectively (Table 1), showing that the dual orientated mesochannels can be accessed by N_2. This confirms the TEM results that MSN-7.5-40 has dual oriented mesochannels interconnected together throughout the nanosphere, and possesses larger mesopore than most MSNs prepared under traditional base medium.

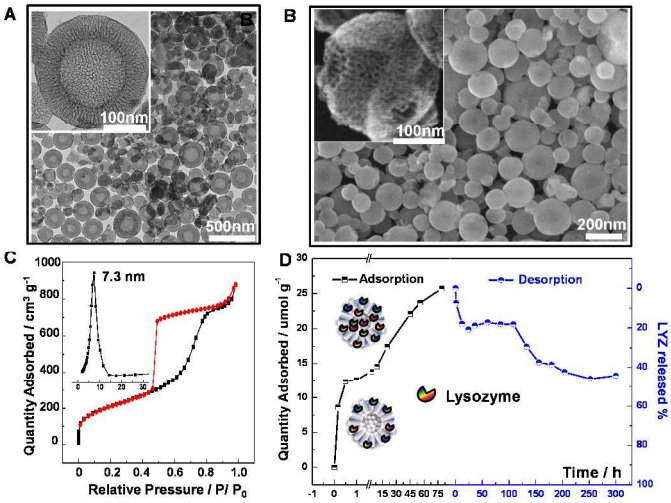

Figure 1. (A) TEM image, (B) SEM image (inset in B is the HR-SEM image of an broken one obtained by grinding during SEM sample preparation), (C) N_2 sorption isotherm of MSN-7.5-40 and (D) adsorption and desorption profiles of LYZ on MSN-7.5-40.

For further characterization of the unique mesostructures and pore orientation, MSN-7.5-40 was used as adsorbent for hen egg white lysozyme (LYZ), which is a globular protein (Mw= 14400 Da) with a dimension of 3.0 × 3.0 × 4.5 nm.[23] It is interesting to notice that two steps could be clearly observed in both the adsorption and desorption kinetic curves (Figure 1D). For the adsorption profile, a platform was reached after a fast adsorption in the initial 0.5 h followed by the second adsorption process. It should be mentioned that the first adsorption process is much faster than the second one. In order to clarify the distribution of LYZ adsorbed on the MSN-7.5-40 at different times, the total N content in MSN-7.5-40 was measured by elemental analysis after adsorption at 0.5 h and 79 h, and data show that N content of MSN-7.5-40 with adsorption time of 0.5 h is lower than that of 79 h (2.5% versus 3.2%), which is consistent with the adsorption capacity results. Then, X-ray photoelectron spectroscopy (XPS) was employed to detect the elemental compositions on the surface layer. The detecting depth of XPS is ca. 10 nm, which is far less than the thickness of the shell (~60 nm). C, N, O, Si elements are clearly found on the MSN-7.5-40 (Figure S3). Notably, the surface N/Si molar ratio of MSN-7.5-40 with LYZ adsorption time of 0.5 h is even higher than that of 79 h (0.54 vs 0.2), which is contrary to the bulky N compositions given by elemental analysis, indicating that the outer shell of MSN-7.5-40 is rich in LYZ at the first 0.5 h. Thus, it could be concluded that LYZ is adsorbed firstly in the shell of MSN-7.5-40, followed by slow diffusion into the core, which explains the two-step adsorption behavior shown in the adsorption profile. Due to the better mass transfer properties of the radial mesochannels, the adsorption takes place on the shell is much faster than that in the core (1h vs 79 h). The LYZ release profile of MSN-7.5-40 also exhibit two steps, corresponding to the fast release from the shell with radial mesochannels and a much slower release from the core with penetrating mesochannels, which further confirms the existence of a two-step adsorption steps presented in the adsorption profile. Liu and coworkers[24] reported a similar three-stage release pattern of ibuprofen using materials with yolk-shell structure. The three-step were corresponding to the release from the external surface, the inner hollow spaces and the mesoporous IBN1 cores respectively, indicating that the unique drug delivery profile is associated with its particular structures. The release behaviour of this dually oriented material provides very promising possibilities in the field of drug delivery system, for the slow release section of the core can extend the time of the drug stayed in body and makes the controlled drug release possible.

Engineering the core and shell thickness of MSNs at different temperatures

It was reported that the synthesis temperature generally affects the swelling behaviour of TMB,[25] which alternatively controls the pore structure and morphology of the mesoporous silicas. Thus, MSN-7.5-70 and MSN-7.5-80 were synthesized under similar conditions to MSN-7.5-40 but with different synthesis temperature. The SEM images show that MSN-7.5-70 and MSN-7.5-80 are nanospheres with particle size of 150~200 nm and have smooth and roughness surface, respectively (Figure 2A). As the TEM and STEM images shown, the two samples have more ordered pore arrangement than MSN-7.5-40, and still maintain the obvious dual orientated mesochannels with the penetrating and radial mesochannels respectively in the core and in the shell (Figure 2B, Figure S4). The TEM image of MSN-7.5-80 looks like sun-flowers with highly ordered penetrating mesopore surrounded by a very thin layer of radial mesochannels near the edge of the nanosphere. Compared with MSN-7.5-40, MSN-7.5-70 and MSN-7.5-80 have relatively larger core size but smaller pore diameter and particle size (Table 1). The N_2 sorption isotherm of MSN-7.5-70 and MSN-7.5-80 exhibit type IV isotherm pattern similar to MSN-7.5-40, but H1 hysteresis loop characteristic of cylindrical mesochannels is observed, which is quite differen from MSN-7.5-40 with cage-like pores (Figure 2C). The above results

suggest that the increase in the synthesis temperature could not only cause the changes in the core size and pore diameter, but also induce the mesostructure evolution from cage-like mesopore to channel-like mesopore.

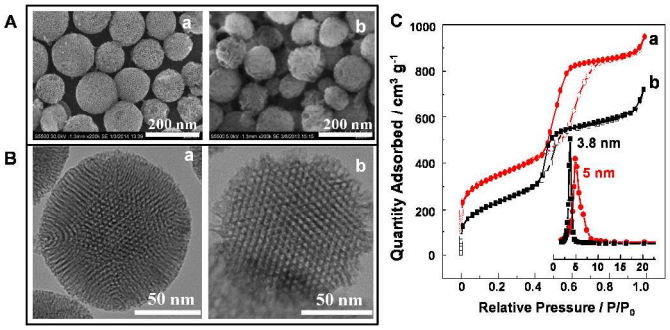

Figure 2. (A) SEM, (B) TEM and (C) N_2 sorption isotherms of (a) MSN-7.5-70 and (b) MSN-7.5-80 with synthesis temperature of 70 and 80 °C, respectively (inset in C are the pore size distribution curves).

Table 1. Synthetic conditions and textural parameters of MSNs with different mesostructure.

Sample	S_{BET} / $m^2 \cdot g^{-1}$	V_{total} / $mL \cdot g^{-1}$ a)	D_{BJH} / nm b)	PSD / Nm c)	Initial rate / $umol \cdot g^{-1} \cdot h^{-1}$ d)	Adsorption Capacity / $umol \cdot g^{-1}$ d)
MSN-7.5-40	765	1.34	7.3	256	51.7	25.71
MSN-7.5-70	896	1.31	5.0	220	94.4	29.46
MSN-7.5-80	844	1.17	3.7	164	62	21.67
MSN-0-70	811	0.98	2.3	142	47.9	19.42
MSN-3-70	910	0.98	2.9	164		
MSN-6-70	745	0.98	3.6	190		
MSN-9-70	912	1.33	6.2	256		
MSN-12-70	908	1.29	5.3	256		
MSN-15-70	597	1.09	9	296		

a) V_{total} is single point adsorption total pore volume at $P/P_0 = 0.99$; b) D_{BJH} is the pore diameter calculated from the BJH theoretical model at the adsorption branch of the sorption isotherms; c) Particle size distribution was determined by dynamic light scattering technique (DLS); d) Initial rate and adsorption capacity is for LYZ adsorption.

The XRD pattern of MSN-7.5-T (T=40, 70, 80) exhibits one diffraction peak in the low 2-theta angle (Figure 3A). As the synthesis temperature decreases, the d spacing shifts to lower 2-theta angle, suggesting the lattice expansion, which is consistent with the pore size distribution based on N_2 sorption characterization. MSN-7.5-70 and MSN-7.5-80 display sharper diffraction peak than MSN-7.5-40, showing that the mesostructure of the former two samples is more ordered than the latter one.

The adsorption of LYZ on MSN-7.5-70 and MSN-7.5-80 were also investigated. For comparison, a control sample, MSN-0-70, was synthesized under similar conditions to MSN-

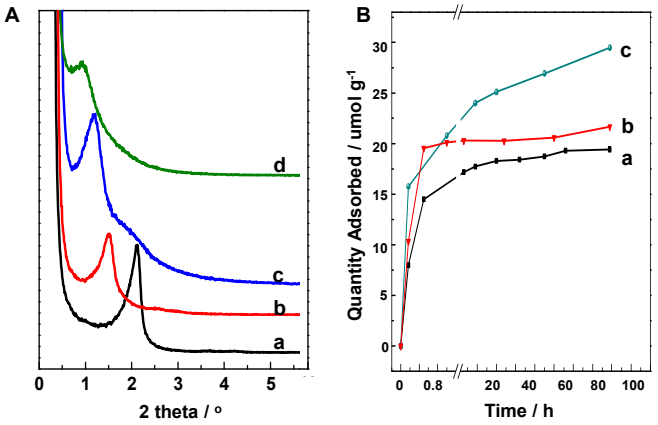

Figure 3. (A) XRD and (B) adsorption profiles of LYZ for (a) MSN-0-70, (b) MSN-7.5-80, (c) MSN-7.5-70 and (d) MSN-7.5-40.

7.5-70 without the addition of TMB. The characterizations of TEM, XRD and N_2 sorption isotherm show that MSN-0-70 possesses penetrating mesochannels of the typical 2D-hexagonal with the small pore diameter of 2 nm (Figure 3A, Figure 4 and Table 1). MSN-7.5-80 and MSN-0-70 display almost the same adsorption curves for LYZ. The adsorption capacity for LYZ increases gradually and reaches a platform at about 1 h. This is because of the thinner shell in MSN-7.5-80 cannot afford the two-step adsorption. For MSN-7.5-70, the LYZ adsorption is very fast in the initial 1 h, followed by a slower adsorption. Similar to MSN-7.5-40, MSN-7.5-70 also exhibits the two adsorption steps but no obvious platform could be observed between the first and the second adsorption step. This is due to the core and shell for MSN-7.5-70 is more intimately connected than that for MSN-7.5-40. The initial adsorption rate decrease in the order of MSN-7.5-70> MSN-7.5-80> MSN-7.5-40> MSN-0-70, showing that MSNs with dual oriented mesochannels show a faster initial rate than those without dual oriented mesochannels, and the MSNs with larger pore diameter have higher adsorption capacity (Table 1). The moderate adsorption rate and adsorption capacity of MSN-7.5-40 is probably due to the larger particle size and the less ordered mesoporous structure of the nanospheres.

The above results suggest that MSNs with dual mesochannel orientation could be facilely synthesized with a wide temperature range. With the increment in the synthesis temperature, the pore diameter decreases, and the structural order increases and 3-D cage-like structure transfers to 2-D hexagonal structure, while the core diameter to shell diameter ratio increases from 1 (MSNs-7.5-40) to 6 (MSN-7.5-80). Engineering the mesochannel orientation and pore diameter of MSNs is very important for their practical applications. Though the MSNs with large pore diameter and with different pore

orientation have been respectively successfully synthesized, the MSNs with dual mesochannel orientation and large pore diameter are seldom reported. The LYZ adsorption experiment indicates that the existence of the dual mesochannel orientation may facilitate the diffusion of the guest molecules throughout the MSNs nanospheres.

The effect of TMB content

Since the first use as a swelling agent for MCM-41 in 1992,[26] 1,3,5-trimethylbenzene (TMB) and its analogues have been widely employed for controlling the pore diameter, mesostructure and morphology of mesoporous materials.[27-32] For the first time, we investigate the mesochannel orientation control during the TMB assisted synthesis process.

The control experiment show that MSN-0-70 synthesized without TMB has penetrating mesochannels, indicating that TMB is one of the important factors for the generation of the unique dually oriented-mesochannels. For investigation the formation mechanism of dual orientated mesochannles, MSN-x-70 samples were synthesized with the different amount of TMB (x) keeping the synthesis temperature at 70 °C. The addition of TMB could enlarge the particle size of MSNs. DLS measurement shows that the particle size of MSN-x-70 samples increases from 142 to 256 nm with the amount of TMB increasing (Figure 4 and Table 1). The SEM characterizations show the similar tendency and all MSN-x-70 samples have spherical morphology (Figure 4B). For MSN-15-70, the existence of microspheres with particle size of 1 um together with nanospheres with particle size of 200 nm was clearly observed in the SEM images (Figure S5). This suggests that large amount of TMB in the synthesis system could cause the phase separation resulting in wide particle size distributions.

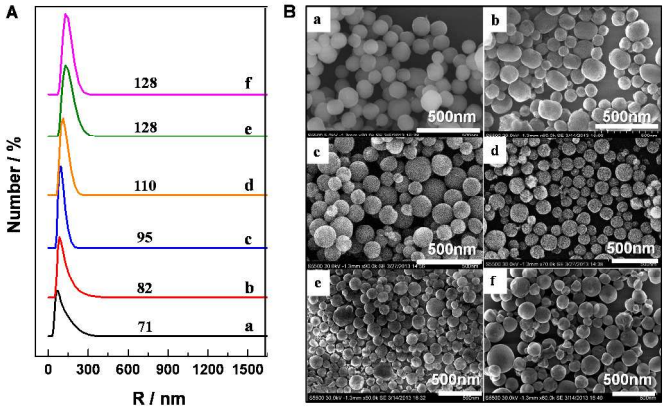

Figure 4. (A) DLS analysis and (B) SEM images of MSN synthesized with different amount of TMB: (a) MSN-0-70, (b) MSN-3-70, (c) MSN-6-70, (d) MSN-7.5-70, (e) MSN-9-70 and (f) MSN-12-70.

The TEM images of MSN-x-70 are shown in Figure 5A. MSN-0-70 prepared in the absent of TMB has the penetrating mesochannels of the typical 2D-hexagonal pore arrangement as we discussed above. MSN-3-70 exhibits similar channel arrangement to MSN-0-70, however, the mesochannels near the edge of the nanosphere twist slightly. The severely mesochannel twisting was observed for MSN-6-70 and the two poles of the spheres were disconnected. As discussed above, MSN-7.5-70 has dual mesochannel orientation with penetrating mesochannels in the core and radial mesochannels in the shell (Figure 2). MSN-9-70 and MSN-12-70 have also dually oriented-mesochannels similar to MSN-7.5-70 but with larger pore diameter and thinner shell. This shows that the length of

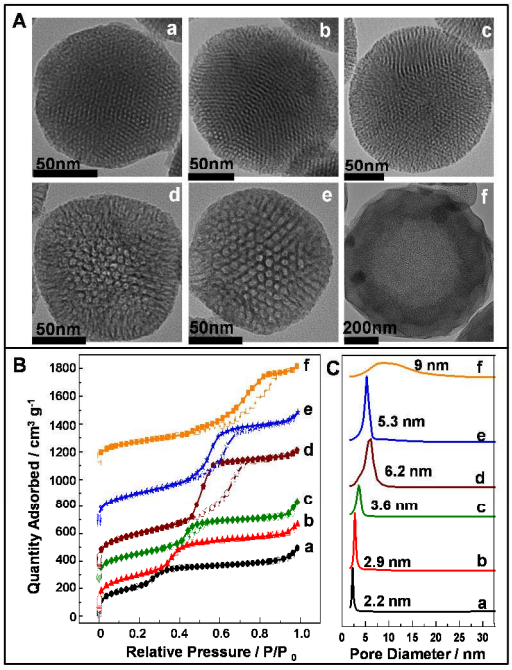

Figure 5. (A) TEM, (B) N_2 sorption isotherm and (C) pore size distribution curves of MSN synthesized with different amount of TMB: (a) MSN-0-70, (b) MSN-3-70, (c) MSN-6-70, (d) MSN-9-70, (e) MSN-12-70 and (f) MSN-15-70.

radial mesochannels in the shell and pore diameter could be adjusted by varying the amount of TMB. However, MSN-15-70 prepared using larger amount of TMB are hollow spheres. All of the materials exhibited type IV isotherm with steep uptake in the adsorption isotherm, showing that all the samples have uniform mesopores (Figure 5B). The H1 hysteresis characteristic of cylindrical channels appears for MSN-x-70 with x≥ 6, indicating the existence of large mesopore. It should be mentioned that MSN-9-70 shows H2 hysteresis loop, suggesting this sample has cage-like mesopore similar to MSN-7.5-40. Further increasing TMB amount, the H1 hysteresis loop appears again for MSN-12-70 and MSN-15-70. As the amount of TMB increases from 0 to 12, the pore diameter increases and reaches the maximum at 6.2 nm (Figure 5C). The BET surface areas of these MSN-x-70 materials are in the range of 597~911 m^2/g (Table 1). The above results show MSNs with dual mesochannel orientation could be obtained using suitable amount of TMB.

Formation mechanism of dually oriented-mesochannels

It has been reported previously that ethanol could initiate a radially oriented mesochannel.[18, 33] In that case, ethanol works as co-solvent, which induces the emergence of radial oriented

mesopores because of the secondary arrangement of CTAB micelles at the interface between the solvent H_2O/EtOH and the primary silica/surfactant aggregates with 2D-hexagonal alignment. Although ethanol was not used in our system, it should be noticed that the hydrolysis of TEOS could produce ethanol and up to 0.2 mol/L could be obtained in the end of the reaction by complete hydrolysis of TEOS. Thus, in the initial step, the hydrolysis and condensation of TEOS around the surfactant micelle leads to the formation of MSNs with penetrating mesochannels. At the same time, the ethanol produced by hydrolysis of TEOS in the system accumulates. When enough ethanol was in the reaction system, it could interact with the surfactant micelles and residue silica species for the formation of silicate species with radial mesochannel. For decreasing the energy, these silicate species tend to deposit on the MSNs with penetrating mesochannles. For comparison, ethanol was added at the very beginning of the synthesis. The TEM images show that larger spheres with only stellate-like channel were obtained, while the core region was hardly to be defined (Figure S6). Thus, it is supposed that the initially formed silicate species with penetrating channels act as nucleus for the ethanol induced radial arrangement of the cylindrical micelles (Scheme 1), which leads to a core-shell-like MSNs with dually oriented-mesostructures. To verify the mechanism, the forming process of MSN-7.5-40 was monitored at different time (Figure 6). It is clearly to be seen that the penetrating channels are developed first, followed by the secondary arrangement of the radial channels, which is corresponding with the formation mechanism proposed. Besides, the effect of ethyl acetate was excluded for the formation of dually oriented-mesochannels. All contribution it made is to improve the dispersity of the nanospheres, as evidenced by the TEM images. The dually oriented-mesochannels already exist when 0 ml ethyl acetate is added into the system (Figure S7A).

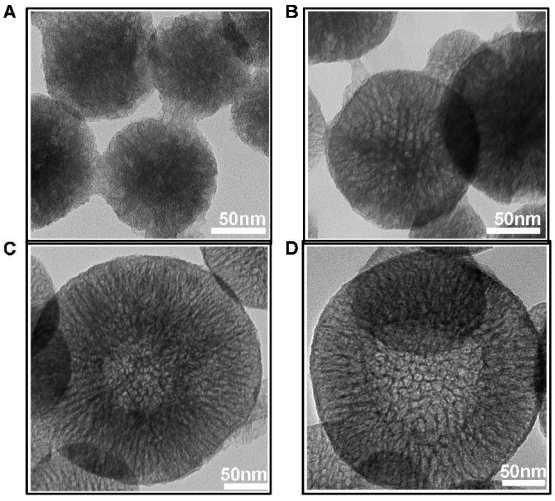

Figure 6. TEM images of MSN-7.5-40 taken out at different times during the formation process: (A) 5 min; (B) 10 min; (C) 30 min and (D) 1 h.

The fact that MSNs prepared without the addition of TMB only has penetrating mesochannles suggests that deposition of the secondary silicate species on the initially formed ones is a kinetic controlled process. Francesca et al. reported that TMB could accelerate the kinetics of formation of the silica solid,[34] thus, the increased hydrolysis rate of TEOS could not only result in a burst of ethanol but also large amount of hydrolyzed silica species. At lower concentration of TMB (TMB/CTAB ratio of 0~7.5), TMB would first diffuse into the hydrophobic micelle core of CTAB to swell the micelle. The expanded micelle size could reduce the charge density of the hydrolyzed Si species, thereby reducing the condensation rate, and provide sufficient time for the secondary self-assembly of CTAB/silica to form the dually oriented-mesostructure. With higher amount of TMB (TMB/CTAB ratio of 7.5~12), TMB could also partly locate around the hydrophilic headgroup of CTAB through a cation-π interaction, thus decrease the polarity of CTAB and favor the condensation for hydrolyzed silica species. If the condensation of hydrolyzed TEOS is too fast, the produced ethanol has not enough time to interact with residue TEOS and surfactant micelles for the formation of silicate species with radial mesochannels. Therefore, MSNs with thinner shell were obtained.

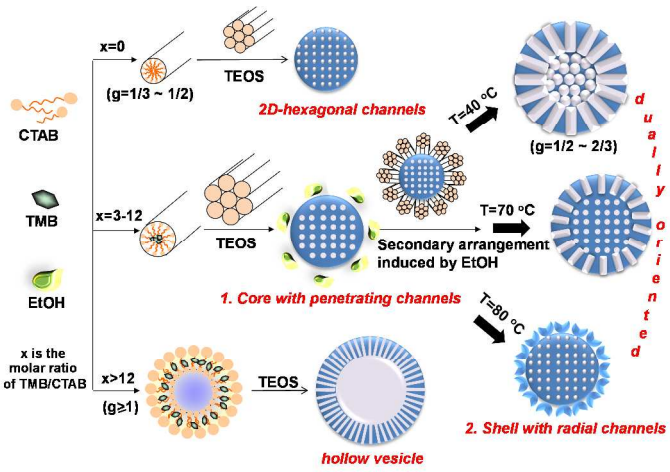

Scheme 1. Schematic illustration of the mechanism for the formation of the MSN-x-Ts with different mesochannel structures.

In addition to control the kinetics of formation of the silica solid, TMB could also affect the packing factors of micelles. In our synthesis system, CTAB forms micelles with hydrophobic tail in the core and hydrophilic head group in the interphase. The hydrolyzed negatively charged silicate species deposit on positively charged micelles and the organic-inorganic co-assembly results in the formation of mesostructure. The MSNs with penetrating mesochannels generally obtained due to the hexagonal mesostructure formed by cooperatively self-assembled CTAB/silica composites. In the presence of TMB, TMB could diffuse into the hydrophobic micelle core through hydrophobic interaction to swell the micelle, thus to influence both the pore diameter and mesostructure. This could explain the pore diameter expansion and the transformation hysteresis from H1 to H2 and again to H1 with the increase in TMB amount. However, the large amount of TMB could form

microemulsion with CTAB, which results in the formation of hollow microspheres. Zhou et al. reported a similar phase transition process in the 1,3,5-triisopropylbenzene (TIPB) and P123 system under acidic conditions.[30]

The influence of the temperature could be straight forwardly elucidated by the hydrolysis and condensation rate of TEOS. The packing factor defined as $g=v/a_0l_c$,[35] where v is the hydrophobic volume of the surfactant; a_0 is the polar head surface area, and l_c is the hydrophobic chain length. In the reaction system, there are larger amounts of unhydrolyzed TEOS at low temperature than at high temperature due to the fact that high temperature facilitates the hydrolysis and condensation rate of TEOS. The hydrophobic TEOS could diffuse into the hydrophobic domain of CTAB to increase the packing parameter g of CTAB by increasing the hydrophobic volume v of CTAB. Moreover, it was reported that lower temperature favours TMB penetrating into the hydrophobic core of the surfactant.[25] Thus, the g value is larger at low temperature than at high temperature. The increase in the g value finally leads to a pronounced phase transformation from the 2-D hexagonal mesostructure to 3-D cage-like mesostructure. The increase in hydrophobic volume of surfactant micelles could also effectively expand the pore diameter. However, further increasing the synthesis temperature to 80 ^{o}C, the hydrolysis and condensation rate of TEOS is too fast to form thick enough shell with radial mesochannel, thus present a sun-flower look. Based on the above discussion, the formation mechanism of different MSNs samples could be outlined as Scheme 1.

Conclusions

Core-shell MSNs with dually oriented-mesochannels and different pore sizes have been successfully synthesized through the radial arrangement of the cylindrical micelles around initially formed silicate species, using TEOS as a precursor and CTAB as a surfactant in the presence of TMB. The core size and shell thickness can be controlled by changing the synthesis parameter such as the synthesis temperature or concentration of TMB. The pore diameter of MSNs can be enlarged to 7.3 nm by lowering the synthesis temperature and increasing TMB content. The ethanol produced from the hydrolyzed TEOS plays an important role for the mesochannel orientation and pore size of resultant MSNs. The LYZ adsorption and release profiles of core-shell MSN with dual oriented mesochannels exhibit unique two steps, corresponding to the fast adsorption/release from the shell with radial mesochannels and a much slower adsorption/release from the core with penetrating mesochannels. Our work provides an efficient method for facilely tuning both the mesochannel orientation and pore size of the MSNs, which would be very useful for potential application in biocatalysis.

Acknowledgements

This work was supported by the National Natural Science Foundation of China (21325313) and the Program Strategic Scientific Alliance between China and the Netherlands (2008DFB50130).

Notes and references

[a] State Key Laboratory of Catalysis, Dalian Institute of Chemical Physics, Chinese Academy of Sciences, 457 Zhongshan Road, Dalian, 116023, China, E-mail: canli@dicp.ac.cn, yangqh@dicp.ac.cn.
[b] Graduate School of the Chinese Academy of Sciences, Beijing, 100049, China.
[c] Department of Chemical Engineering, Curtin University, Perth, WA 6845, Australia

† Electronic Supplementary Information (ESI) available. See DOI: 10.1039/b000000x/

1 D. Y. Zhao, J. Y. Sun, Q. Z. Li, G. D. Stucky, *Chem. Mater.* 2000, **12**, 275-279.
2 H. I. Lee, J. H. Kim, G. D. Stucky, Y. F. Shi, C. Pak, J. M. Kim, *J. Mater. Chem.* 2010, **20**, 8483–8487.
3 X. L. Ji, K. T. Lee, M. Monjauze, L. F. Nazar, *Chem. Commun.* 2008, 4288–4290.
4 T. Yu, A. Malugin, H. Ghandehari, *ACS Nano.* 2011, **5**, 5717–5728.
5 P. Linton, V. Alfredsson, *Chem. Mater.* 2008, **20**, 2878–2880.
6 M. H. Kim, H. K. Na, Y. K. Kim, S. R. Ryoo, H. S. Cho, K. E. Lee, H. Jeon, R. Ryoo, D. H. Min, *ACS Nano.* 2011, **5**, 3568–3576.
7 G. Lelong, S. Bhattacharyya, S. Kline, T. Cacciaguerra, M. A.Gonzalez, M. L. Saboungi, *J. Phys. Chem. C* 2008, **112**, 10674–10680.
8 L. B. Han, Y. Zhou, T. He, G. S. Song, F. Wu, F. R. Jiang, J. Q. Hu, *J. Mater. Sci.* 2013, **48**, 5718–5726.
9 J. L. Gu, K. Huang, X. Y. Zhu, Y. S. Li, J. Wei, W. R. Zhao, C. S. Liu, J. L. Shi，*J. Colloid Interface Sci.* 2013, **407**, 236 - 242.
10 H. J. Dong, J. D. Brennan, *J. Mater. Chem.* 2012, **22**, 13197.
11 S. G. Wang, C. W. Wu, K. Chen, V. S. Y. Lin, *Chem. Asian J.* 2009, **4**, 658 – 661.
12 Q. Cai, Z. S. Luo, W. Q. Pang, Y. W. Fan, X. H. Chen, F. Z. Cui, *Chem. Mater.* 2001, **13**, 258-263.
13 R. I. Nooney, D. Thirunavukkarasu, Y. M. Chen, R. Josephs, A. E. Ostafin, *Chem. Mater.* 2002, **14**, 4721-4728.
14 Y. Han, J. Y. Ying, *Angew. Chem. Int. Ed.* 2005, **44**, 288 –292.
15 F. Gao, P. Botella, A. Corma, J. Blesa, L. Dong, *J. Phys. Chem. B* 2009, **113**, 1796–1804.
16 D. C. Niu, Z. Ma, Y. S. Li, J. L. Shi, *J. Am. Chem. Soc.* 2010, **132**, 15144-15147.
17 T. Suteewong, H. Sai, R. Hovden, D. Muller, M. S. Bradbury, S. M. Gruner, U. Wiesner, *Science* 2013, **340**, 337-341.
18 B. Tan, S. E. Rankin, *J. Phys. Chem. B* 2004, **108**, 20122-20129.
19 J. B.S. Ng, P. O. Vasiliev, L. Bergström, *Micropor. Mesopor. Mater.* 2008, **112**, 589–596.
20 Y. L. Chen, M. Xiao, W. Zhuang, Y. Li, B. Z. Li, Y. G. Yang, *Chin. J. Chem.* 2012, **30**, 1582—1588.
21 V. Polshettiwar, D. Cha, X. X. Zhang, J. M. Basset, *Angew. Chem. Int. Ed.* 2010, **49**, 9652 –9656.
22 K. Zhang, L. L. Xu, J. G. Jiang, N. Calin, K. F. Lam, S. J. Zhang, H. H. Wu, G. D. Wu, B. Albela, L. Bonneviot, P. Wu, *J. Am. Chem. Soc.* 2013, **135**, 2427-2430.

23 J. Liu, S. Y. Bai, Q. R. Jin, H. Zhong, C. Li, Q. H. Yang, *Langmuir* 2012, **28**, 9788-9796.
24 J. Liu, S. Z. Qiao, S. B. Hartono, G. Q. Lu, *Angew. Chem. Int. Ed.* 2010, **49**, 4981 –4985.
25 J. Fan, C. Z. Yu, J. Lei, Q. Zhang, T. C. Li, B. Tu, W. Z. Zhou, D. Y. Zhao, *J. Am. Chem. Soc.* 2005, **127**, 10794-10795.
26 J. S. Beck, J. C. VartUli, W. J. Roth, M. E. Leonowicz, C. T. Kresge, K. D. Schmitt, C. T. W. Chu, D. H. Olson, E. W. Sheppard, S. B. McCullen, J. B. Higgins, J. L. Schlenker, *J. Am. Chem. Soc.* 1992, **114**, 10834-10843.
27 Y. Hoshikawa, H. Yabe, A. Nomura, T. Yamaki, A. Shimojima, T. Okubo, *Chem. Mater.* 2010, **22**, 12–14.
28 S. K. Jana, R. Nishida, K. Shindo, T. Kugita, S. Namba, *Micropor. Mesopor. Mater.* 2004, **68**, 133–142.
29 G. W. Zhou, Y. J. Chen, J. H. Yang, S. H. Yang, *J. Mater. Chem.* 2007, **17**, 2839-2844.
30 A. Fukuoka, I. Kikkawa, Y. Sasaki, A. Shimojima, T. Okubo, *Langmuir* 2009, **25**, 10992–10997
31 J. X. Zhang, X. Li, J. M. Rosenholm, H. C. Gu, *J. Colloid Interface Sci.* 2011, **361**, 16–24.
32 T. Lu, X. D. Yao, G. Q. (Max) Lu, Y. H. He, *J. Colloid Interface Sci.* 2009, **336**, 368–373.
33 S. Q. Liu, P. Cool, O. Collart, P. V. D. Voort, E. F. Vansant, O. I. Lebedev, G. V. Tendeloo, M. H. Jiang, *J. Phys. Chem. B* 2003, **107**, 10405-10411.
34 M. F. Ottaviani, A. Moscatelli, D. D. Giscard, F. D. Renzo, P. J. Kooyman, B. Alonso, A. Galarneau, *J. Phys. Chem. B* 2004, **108**, 12123-12129.
35 H. P. Lin, C. Y. Mou, *Acc. Chem. Res.* 2002, **35**, 927-935.